

# Seismicity acceleration and clustering before the 2015 $M_w$ 7.9 Gorkha earthquake, Nepal

B. Gardonio \* <sup>1,2</sup>, L. Bollinger <sup>1</sup>, M. Laporte <sup>2</sup>, J. Vergne <sup>3</sup>, H. Lyon-Caen <sup>4</sup>, L.B. Adhikari <sup>5</sup>

<sup>1</sup>CEA, DAM, DIF, 91297 Arpajon, France, <sup>2</sup>Univ Lyon 1, ENSL, CNRS, LGL-TPE, F-69622, Villeurbanne, France, <sup>3</sup>IPGS-EOST, CNRS/Université de Strasbourg, 67000 Strasbourg, France, <sup>4</sup>Laboratoire de Géologie, CNRS UMR 8538, Ecole normale supérieure, PSL University, 75005 Paris, France, <sup>5</sup>Department of Mines and Geology, Nepalese National Earthquake Monitoring and Research Centre, Lainchaur, Kathmandu, Nepal

**Author contributions:** *Conceptualization:* B. Gardonio, L. Bollinger, J. Vergne, H. Lyon-Caen, M. Laporte, L. B. Adhikari. *Formal analysis:* B. Gardonio, L. Bollinger, J. Vergne. *Investigation:* B. Gardonio, L. Bollinger, J. Vergne, H. Lyon-Caen. *Writing:* B. Gardonio, L. Bollinger. *Visualization:* B. Gardonio, L. Bollinger, M. Laporte. *Writing - review & editing:* B. Gardonio, L. Bollinger, M. Laporte, H. Lyon-Caen.

**Abstract** In the last decade, several observations of peculiar seismic and geodetic phases preceding large earthquakes have been documented. Despite being a posteriori, these observations provide a better understanding of the processes involved in the nucleation of earthquakes. In this study, we investigate the foreshocks and the pre-seismic phase of the  $M_w$  7.9 25 April 2015, Gorkha earthquake in Nepal by applying a matched-filter technique to its nucleation zone. We use the seismic signals of 1851 local earthquakes and the continuous signal recorded at the nearest station for the 6 years preceding the mainshock. The pre-seismic phase depicts a long-term increase of seismicity rate and several seismic swarms less than 20 km away from the mainshock epicenter. The longest swarm occurs one month before the Gorkha earthquake, lasts two weeks and consists of 38 repetitive earthquakes located at the northwestern edge of the rupture zone. Another increase in seismicity rate starts six days before the mainshock and includes small foreshocks that develop less than 10 kilometers from the future earthquake hypocenter. These observations suggest that the Gorkha earthquake was preceded by a pre-seismic phase related to a possible initiation of a slow slip with fluids involved at the northwestern boundary of the rupture zone.

**Non-technical summary** In the last decade, several observations of phases preceding large earthquakes have been documented. In 2015, on the 25th of April, a magnitude 7.9 struck Nepal resulting in more than 9000 fatalities. In this study, we analyse small earthquakes in the nucleation area of this large earthquake and find that seismic activity gradually increased over six years, especially in the weeks preceding the mainshock. About a month before the earthquake, a cluster of small, repeating earthquakes occurred near the rupture nucleation zone, and more small events occurred just days before the mainshock. These patterns suggest that the earthquake may have been preceded by a slow slip of the fault, possibly influenced by underground fluids. While these signals were only recognized after the earthquake, they offer important clues about the nucleation processes at stake before major earthquakes.

## 1 Introduction

Nepal is located on one of the largest and fastest-slipping continental megathrusts on Earth, the Main Himalayan Thrust (MHT) activated by the continental subduction of the India plate beneath the Tibetan plateau. This tectonic setting results in large devastating earthquakes (Bilham, 2019; Avouac, 2003). These major earthquakes ruptured the surface, generating pluri-metric seismic scarps as progressively revealed by palaeo-seismological excavations (Wesnousky et al., 2017; Riesner et al., 2023). One of these historical earthquakes occurred in 1833 (magnitude estimated 7.7). It was fortunately preceded by two foreshocks, felt in Kathmandu 5 hours and 15 minutes before the mainshock, that drove people outdoors (Bilham, 1995). However, the mechanisms operating at depth, especially along the deeper extension of the ruptured

fault—thought to be the origin of the earthquake nucleation—remain unclear.

The  $M_w$  7.9 Gorkha earthquake, on 25 April 2015, is the first major Himalayan event recorded by a permanent and modern network located above the rupture zone. This earthquake nucleated near the village of Barpak in the Gorkha district. The rupture extended eastward for approximately 60 seconds across a 50-km-wide by 140-km-long area, with the maximum coseismic slip estimated to be around 7 meters, occurring north of Kathmandu (Fig. 1, Avouac et al., 2015; Galetzka et al., 2015; Grandin et al., 2015; Kobayashi et al., 2015; Lindsey et al., 2015). The post-seismic slip dominated by afterslip has been located in the down-dip part of the mainshock rupture (Gualandi et al., 2017; Wang et al., 2017). The analysis of the numerous aftershocks has highlighted the structural complexities of this area (Adhikari et al., 2015; Bai et al., 2019; Hoste-Colomer et al., 2017; Wang et al., 2017; Mendoza et al., 2019; Ya-

Production Editor:  
Gareth Funning  
Handling Editor:  
Stephen Hicks  
Copy & Layout Editor:  
Théa Ragon

Received:  
September 18, 2024  
Accepted:  
April 24, 2025  
Published:  
May 5, 2025

\*Corresponding author: blandine.gardonio@univ-lyon1.fr

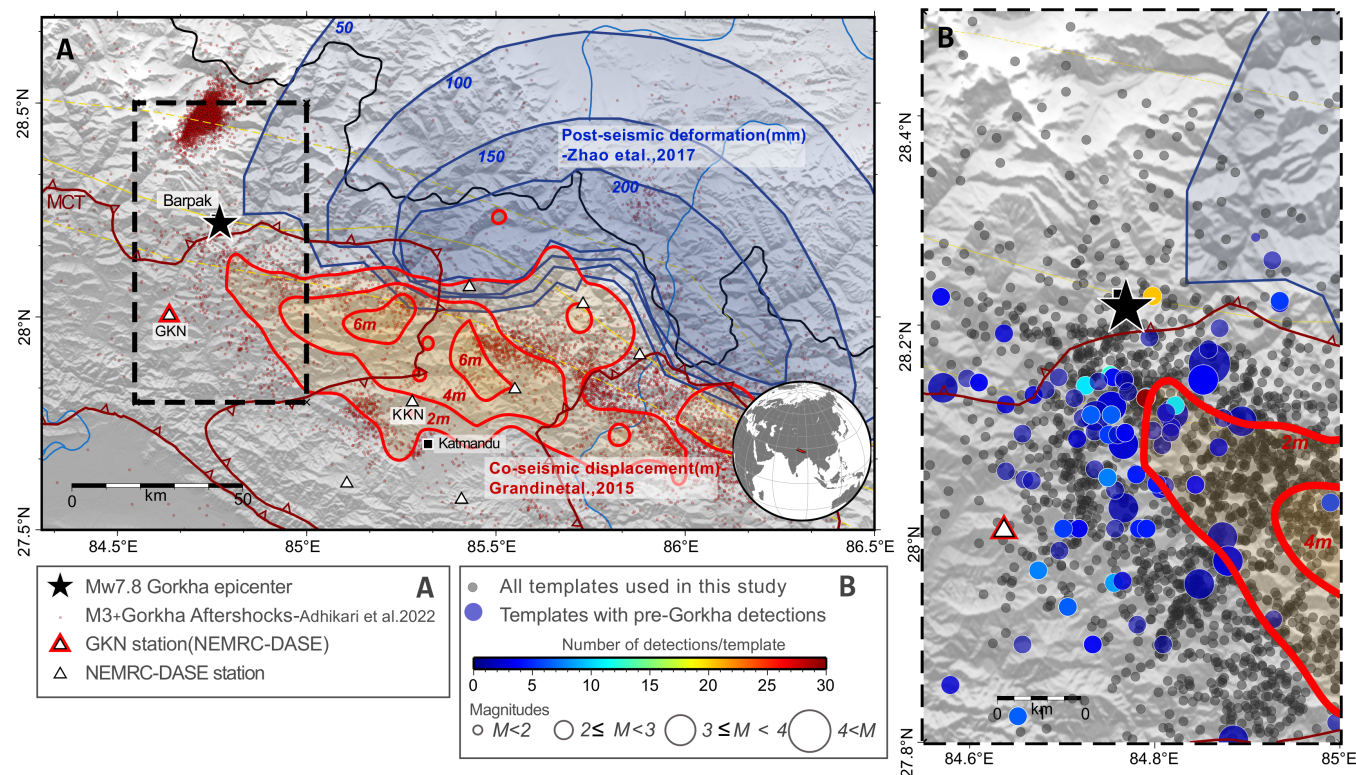


**Figure 1** A: Location of earthquakes and network stations. Red dots show the  $M \geq 3$  aftershocks earthquake (Adhikari et al., 2022). The red contours show the seismic slip with 2m intervals starting at 2m (Grandin et al., 2015). Contours of afterslip are shown in blue (Zhao et al., 2017). The black star indicates the Gorkha earthquake epicenter. Black triangles indicate the NEMRC stations and the red triangle indicates the GKN station used in this study. Black crosses indicate the location of the cross-section in Fig. 7. The yellow line indicates the coupling limit of the Main Himalayan Thrust (MHT) from Lindsey 2018 and the dotted line is the 95% confidence interval (Lindsey et al., 2018). B: In this study, we focus on the initiation part of the rupture zone taking earthquakes that occur both before and after the Gorkha earthquake as templates (all circles) at the western edge of the rupture. The colored circles show the templates that have detected new earthquakes during this study, colored with their number of detections.

mada et al., 2019; Letort et al., 2016; Baillard et al., 2017; Adhikari et al., 2022; Koirala et al., 2023). The correspondence between the 1833 and Gorkha earthquakes in areas of large intensity and their similar magnitudes indicate that the same section of the MHT was active at that time. Unfortunately, unlike the 1833 earthquake, the population did not experience large foreshocks before the Gorkha earthquake (Martin et al., 2015).

There have been several, made a posteriori, observations of a pre-seismic phase before large earthquakes using seismicity, either in subduction zones (Kato et al., 2012; Ruiz et al., 2014; Bouchon et al., 2013, 2016; Gardonio et al., 2019; Bouchon et al., 2022), or in crustal environment (Bouchon et al., 2011; Gardonio et al., 2018), although this pre-seismic phase is not always observed and is highly debated (Gomberg, 2018) and anomalous foreshock behavior may be observed only when analyzing microseismicity (Mignan, 2014). A first analysis of the micro-seismicity has suggested the increase in seismicity rate 3 to 4 days prior to the Gorkha earthquake (Huang et al., 2017). However, the stations used were primarily located over 200 km away from Gorkha, mostly in Tibet, which likely resulted in the exclusion of smaller seismic events occurring near the epicenter.

In this study, we address the question of the pre-seismic phase of the Gorkha earthquake by using the

nearest station of the National Earthquake Monitoring and Research Center (NEMRC) from the Department of Mines and Geology (DMG) network and apply a matched-filter technique. We use 1851 templates, i.e. signals of local earthquakes located within 50 km from the epicenter (Fig. 1). Using this new catalog, we describe the pre-seismic phase of the Gorkha earthquake that occurred in a continental subduction and propose different models to explain our observations.

## 2 Data

The NEMRC network is composed of short period and broadband stations sampling at 50Hz, distributed throughout Nepal. The closest stations from the Gorkha rupture initiation are GKN and KKN (Fig. 1). However, the two stations were affected by several gaps and, because of its distance from the nucleation zone, the KKN station did not capture all the templates that were recorded by the GKN station. Therefore, we focus the analysis using the GKN station only. The GKN station lies 30 km south of the epicentre of the Gorkha Earthquake, above the MHT (red triangle in Fig. 1A). It is a ZM500 instrument with a vertical component, 1 Hz velocimeter with a flat response from 2 Hz to 100 Hz (Lar-

sonnier et al., 2019). The Gorkha seismic station site was installed at the top of a hill for radio-transmission through a 6 meter-high antenna to avoid any anthropogenic noise and the noise of rivers during the monsoon.

We use the records from this short period -vertical component- station to search for micro-earthquakes that remained undetected by analysts, in order to complement the time structure of the seismicity (colored circles in Fig. 1B). Note that the signals of station GKN were unusable from the 26th of March 2009 to the 5th of September 2009 and from January 2011 to November 2013 because of several problems with the recorder electrical cables. Additionally, short-term duration gaps also occurred in 2014 and 2015. In total, 50% of the data is available for GKN station from 2009 up to Gorkha earthquake occurrence time. See the power spectral density plots for GKN in 2014 (Supplementary Figure S1) and 2015 (Supplementary Figure S2).

By first looking at the continuous recording of the GKN station at the time of the mainshock, we find an earthquake of magnitude estimated at 1.3 (equation 1) that occurred only 28s before the mainshock (Supplementary Figure S3). This event has a S-minus-P travel time of 2.86s suggesting that it happened at 23 km from GKN, assuming a  $V_p/V_s$  of 1.75 and a  $V_p$  around 6 km/s, consistent with the local velocity model (Pandey, 1985). Note that the record signal saturated during the mainshock and an S-time arrival cannot be determined. An event preceding the mainshock is also visible in the seismic signal at KKN, located further east, with a P-wave arrival time difference between KKN and GKN of 6.8s, identical to the Gorkha earthquake, suggesting that this foreshock occurred in close proximity to the epicenter (Supplementary Figure S4).

### 3 Methods

We search more systematically for micro-seismic events near the hypocenter of the Gorkha earthquake using the ObsPy template matching code (`obsypy.signal.cross_correlation`, Beyreuther et al., 2010). We use 1851 templates, occurring between January 2009 and May 2016 (gray and colored circles in Fig. 1b). We use the continuous signal from 2009 to the Gorkha earthquake to compute the correlation between templates and continuous signals in a frequency band of 2-15Hz, taking an 8-seconds window starting 1 second before the P-wave arrival time. We chose a coherency of 0.7 as a threshold for detection but tested higher values (Supplementary Figure S5). We checked every detection by eye to remove spurious ones.

The magnitude of template events, provided by the NERMC, are local ( $M_l$ ). The magnitudes of the newly detected events are calculated during the correlation computation based on the maximum amplitude (A) ratio between the detected event, and its template event, as:

$$m_{detection} = m_{template} + \frac{4}{3} * \log_{10}\left(\frac{A_{detection}}{A_{template}}\right) \quad (1)$$

We tested it using a pair of nearby templates that de-

tected each other and have local magnitudes of  $m_{lA}=2.4$  and  $m_{lB}=2.8$  and the relative magnitudes obtained  $m_A=2.7$  and  $m_B=2.8$ .

The distance between a given template and its detections is inherently very small due to the similarity of the waveforms. The example of earthquakes detected in 2010 with a coherency threshold of 0.7 shows that, when aligning on the S wave arrivals, the P waves are not well aligned and their arrivals vary within 0.32 seconds (Supplementary Figure S6). Assuming a P wave velocity of 6 km/s, it corresponds to a distance of about 2 km which is below the location uncertainty for the Nepalese catalog, with a median of the long axis of uncertainty ellipse at 5 km (Laporte, 2022).

We therefore consider that the hypocenters of the newly detected earthquakes are the same as their corresponding templates.

The precise hypocentral location of the template could be enhanced through the implementation of specific relocation technique. We use hypo71 using the local velocity model (Pandey, 1985). The initial weight for P and S phases is 1 and 0.5 respectively. In addition, a distance weighting of 1 below 100 km and linearly decreasing to 0 between 100 and 200 km is applied.

### 4 Results

Of the 1851 templates used, only 143 detected new earthquakes (colored circles in Fig. 1B). Among these 143, 103 occurred before the mainshock and 40 after. We obtain a total of 492 detected earthquakes (including the 103 templates that occurred between January 2009 and the Gorkha earthquake). Supplementary Figure S7 shows an example of detected earthquakes and their stack.

In this study, we define as a cluster a group of at least 5 earthquakes detected by the same template. We sort the detected earthquakes according to their epicentral distance to the Gorkha earthquake (Fig. 2). Only 48 earthquakes were detected at distances larger than 30km from the epicenter (Fig. 2a). Note that the total number of detections increases when getting closer to the epicenter (Fig. 2b and c).

From November 2013 to the Gorkha earthquake, the detections are mainly located from 0 to 20 km : 45% of the earthquakes located from 0 to 20 km away from the epicenter occur during that period of time while only 20% of the 20-30 km earthquakes occur during this period (Fig. 2b and c). We focus on these two zones in the following.

For earthquakes located 20-30 km away from the epicenter, the sequence can be divided into 6 periods (A-F in Fig. 2b and detailed in Supplementary Figure S8). Three of them are particularly intense: 1) period A in January 2009 with three clusters of 10, 11 and 15 earthquakes detected by three different templates (Supplementary Figure S8A), 2) period C: on the 26th of August 2010, lasts 34 hours with two main clusters of 10 and 12 earthquakes detected by two, close-by, earthquakes (Supplementary Figure S8C), 3) period D: from the 2010/12/8 to the 2010/12/10, consists of two main clusters: 9 and 11 earthquakes detected by 2 different

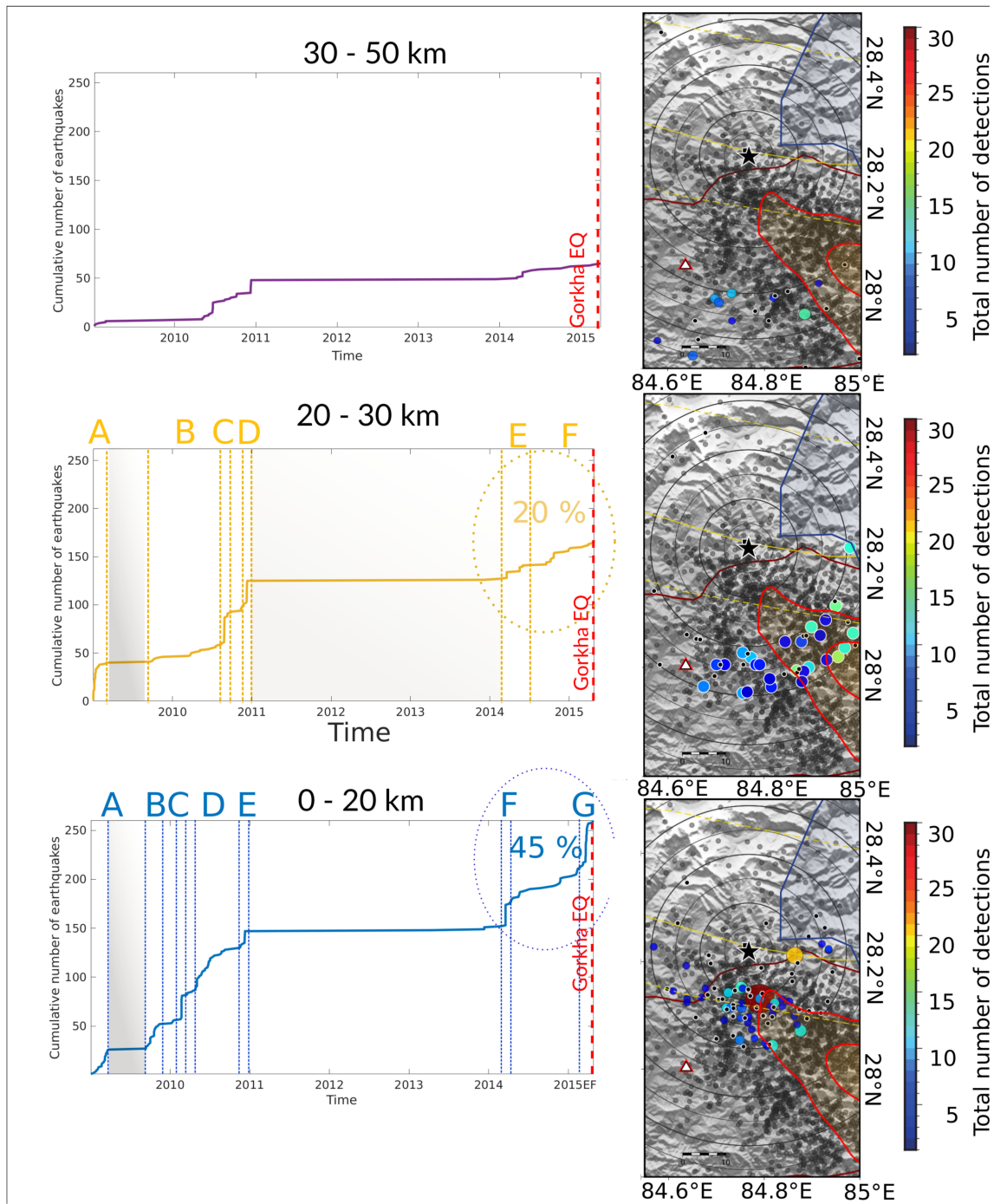


**Figure 2** Cumulative number of detected earthquakes with time according to their epicentral distance from Gorkha earthquake and their location. a: from 30 to 50km, b: from 20 to 30km, c: from 0 to 20 km. The maps show the template locations that detected these earthquakes color coded with their total number of detection. Grey areas indicate gaps in the continuous data. Letters above the cumulative number of earthquakes refer to the periods shown in the snapshots (Supplementary Figure S8 for 20-30 km and S9 for 0-20 km). Note that between 0-20km, 45% of the detections occur after 2014 while only 20% of the detections occur between 20-30km for the same period.

templates and lasts about two days and a half (Supplementary Figure S8D).

Earthquakes detected between 0-20 km from the epicenter show 7 periods of seismicity rate increase (Fig. 2c, detailed in Supplementary Figure S9). Periods A and B present similar seismicity rates with a total of 51 earthquakes located south of the Gorkha epicenter (Supplementary Figure S9A and B). Periods C, E, F and G show very sudden increases in seismicity rate. Period C gathers 21 earthquakes starting on February 21

2010, at 23:00, and lasting 48 hours (yellow dot in Supplementary Figure S9C). This period contains a group of 16 earthquakes, that are all detected by the same template in 3.5 hours, 14 of them in only an hour (Supplementary Figure S10). The cross-correlation values are particularly high and the relative time delays low for the last ten events in the group. Note that the relative magnitudes are small and similar.

Period F corresponds to a large cluster of 28 earthquakes occurring in just one hour on the 19/03/2014

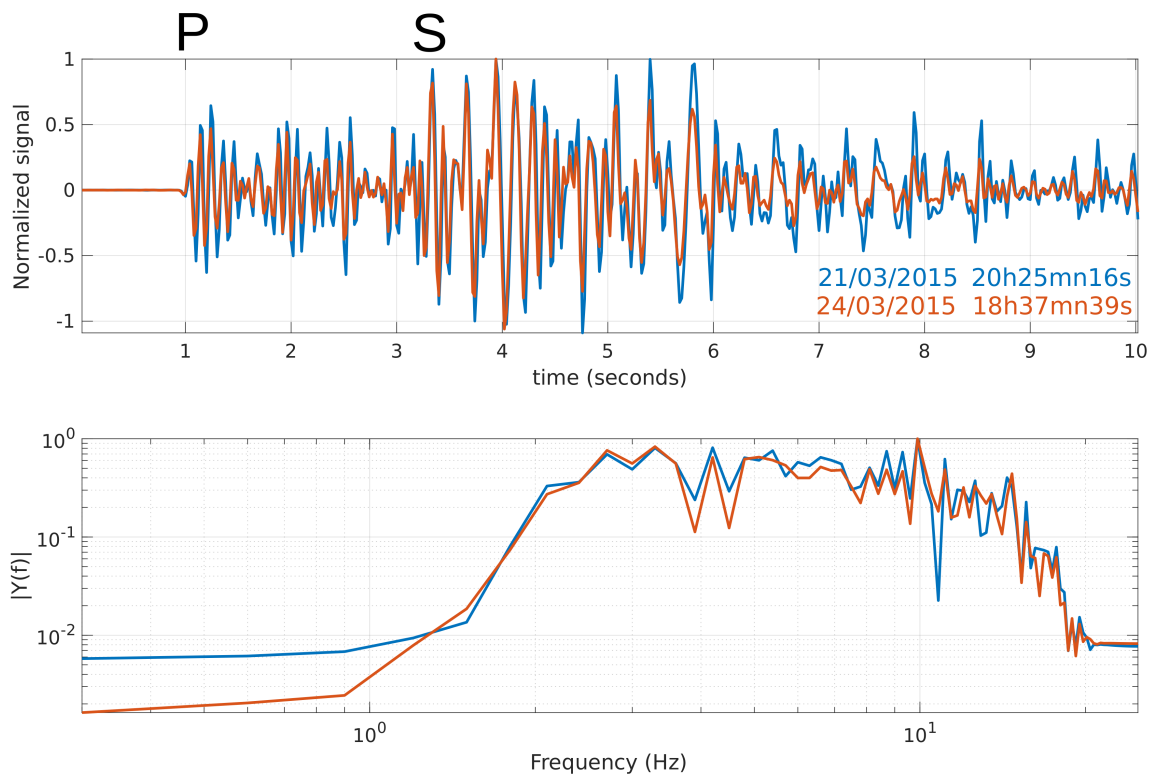


**Figure 3** Top: Superposition of the band-pass filtered (2-20Hz) records of the two largest earthquakes in the sequence of Fig. 4 (magnitude 2.7 and 3, large red circle collocated with a blue one on Fig. 2c-map) that were already in the NERMC catalog, from which 36 new earthquakes were detected. The second waveform has been shifted in time by the time increment that maximizes the cross-correlation of the two signals. Bottom: Comparison of the normalized spectra of the records filtered with a band-pass between 2-20Hz.

between 00h35 and 01h39, mainly detected by three templates (Supplementary Figure S9F). The inter-correlation values of this group range from 0.8 to 1 with a mean of 0.91 (Supplementary Figure S11). Some events in the groups have very large cross-correlation values, with a mean of 0.95, possibly indicating that they are repeating earthquakes. Again, there is no dominant magnitude in this very short sequence.

The most significant cluster in number of earthquakes and in duration occurs one month before the Gorkha mainshock, during period G. It starts on the 20th of March 2015 and lasts 13 days. These earthquakes are detected by two, very close-by templates, 10 km away from the Gorkha epicenter (superposed red, magnitude 2.7 and blue, magnitude 3, dots in Supplementary Figure S9G) that occur during this sequence. Their magnitudes indicate that their ruptures could have a patch size of about 200-300m. Furthermore, the two template waveforms are very similar when superimposed, and their spectra show the same complexity, suggesting that they are very likely co-located (Fig. 3).

The cross-correlation values between the earthquakes of this cluster (i.e. the two templates and their detections) are high (Fig. 4a). The delay values range from -0.02 to 0.02s (Fig. 4b). The S-minus-P traveltime is 2.18s (i.e., a distance of about 17.5km from the GKN station) and is very similar for all the earthquakes within the cluster (Fig. 4c and d). Unlike previous increases in seismicity rate that have durations of a few hours, this

sequence lasts 13 days and contains three main seismic bursts (Fig. 4e): (1) 7 earthquakes with magnitude close to 0 in 10 hours, (2) another burst of 10 earthquakes that starts with a magnitude 2.7 that is one of the detecting template (in red in Fig. 3), (3) 7 earthquakes that contains the second template of magnitude 3 (in blue in Fig. 3).

This cluster of earthquakes is located at the western tip of the inverted 2m coseismic slip contour, where the rupture initiated (Grandin et al., 2015, Supplementary Figure S9G). We take the 13 most resembling earthquakes (coherency higher than 0.98) of that cluster and superimposed their waveforms (Supplementary Figure S12). We see that they present the same complexities in their P and S waves but also coda waves and that they are perfectly superimposed with a high probability for them to be repeating earthquakes.

Lastly, three earthquakes occurred during period G from April 21, 2015 to the mainshock, including the small foreshock that occurred only 28s before the mainshock close to the rupture initiation location (Supplementary Figure S3).

In summary, by applying the template-matching technique at the GKN station, we identify 492 earthquakes, with 260 of them occurring within 20 km of the epicenter, primarily from November 2013 until the Gorkha earthquake. We observe a cluster of earthquakes that begins one month prior to the mainshock and lasts for 13 days. During the period from April 14

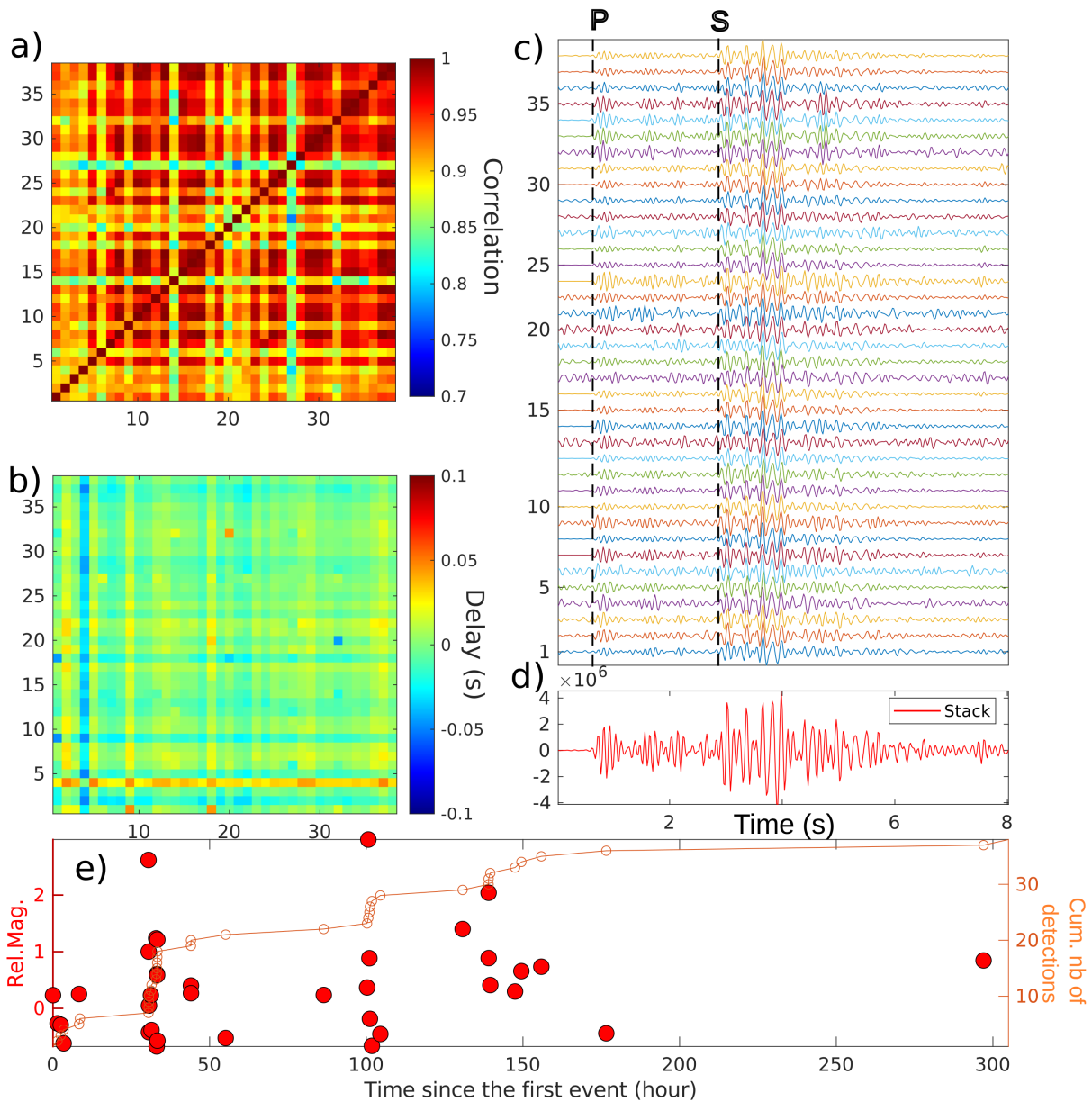


**Figure 4** Group of 38 earthquakes occurring from the 20/03/2015 to the 02/04/2015, detected by two, very close by, templates. a) Cross-correlation matrix between the earthquakes b) delay matrix (in s); c) waveforms of the detected earthquakes with their stack at the bottom, d) cumulative number and relative magnitude of events with time with the zero at the occurrence of the first event of the cluster. The cross-correlation values are particularly high and the relative time delays low for thirteen earthquakes in the group Supplementary Figure S12.

to April 25, we detect 6 earthquakes at an average distance of 21 km from the epicenter. (Huang et al., 2017) identified 6 earthquakes within a 500 km radius from the epicenter on April 21–22. The south-eastern part of the studied area that corresponds to the westernmost rupture zone of the earthquake, is more active in 2009–2010 with numerous clusters of seismicity (cyan and yellow dots in Fig. 5a) while it stops being active during the November 2013–Gorkha period (Fig. 5b).

### 5 Statistical Analysis

To evaluate if the seismicity rate increases in the 0–20 km distance range from the epicenter is due to background or dependent seismicity, we performed a

declustering analysis (Gardner and Knopoff, 1974; Zaliapin and Ben-Zion, 2022; Marsan and Wyss, 2011).

We use the maximization-expectation algorithm developed in Marsan and Lengline (2008) and took into account only the time intervals with continuous data and applied to our catalogue cut at magnitude 0 (Fig. 6).

To decluster the catalogue of our newly detected earthquakes, we must consider (1) the gap in the data and (2) the inability to locate the microearthquakes identified through template matching, as we are working with only one station. It is therefore biased to use distance-based methods, as we assume that a detected earthquake corresponds to its template location. In this case, the distance between two events would be zero, which causes algorithms like those of Zaliapin and Ben-

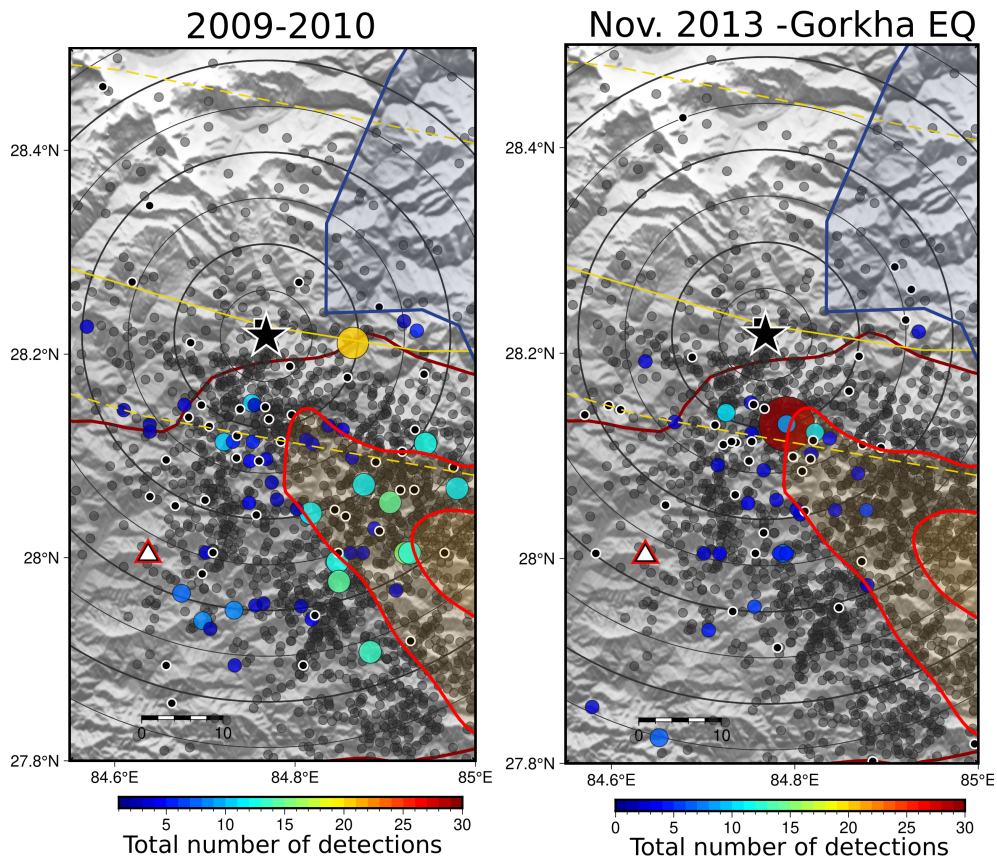


**Figure 5** Location of templates that have detected new earthquakes during the a) 2009-2010 period and b) November 2013-Gorkha earthquake period, color and size give the number of detections during these periods. Legend is the same as in Fig. 1A and B except for the size of the dots that is proportional to the number of detections here.

Zion (2022) to struggle. To address this issue, we modeled our dataset using the ETAS model (Ogata, 1988). We invert for the background seismicity rate  $\mu$  and the pre-productivity factor  $K$ . Careful consideration is required when making assumptions about other parameters, such as the  $p$ -value, the  $\alpha$ -parameter and  $c$ . For example, the  $p$ -value is expected to be close to 1, typically ranging from 0.8 to 1.2 (Utsu et al., 1995; Hainzl and Marsan, 2008). In this study, we set  $p = 1$ . The  $\alpha$ -parameter typically ranges from 1.5 to 2.5 (Hainzl et al., 2013; Nandan et al., 2017, and references therein) and we set  $\alpha = 2$  here. Lastly, we fix  $c$ , the time at which the maximum of the inter-event time density is observed to be equal to 0,0035 day (i.e. 5 minutes).

We see that the final acceleration located close to the epicentral area of the Gorkha earthquake is a persistent part of the background seismicity.

We can measure the significance of the seismicity rate change for the earthquakes located in the 0-20 km distance bin from the epicenter by applying the Z statistics analysis (Habermann, 1981) which is a measure of the difference between the expected number and the actual number of earthquakes observed as:

$$Z = \frac{N_a \Delta t_b - N_b \Delta t_a}{\sqrt{N_a \Delta t_b^2 + N_b \Delta t_a^2}} \quad (2)$$

with  $N_b$  and  $N_a$  the number of earthquakes that occur in time intervals  $\Delta t_b$  and  $\Delta t_a$ , respectively before and after the considered time limit. It evaluates the difference between two means, that is the mean rates before and

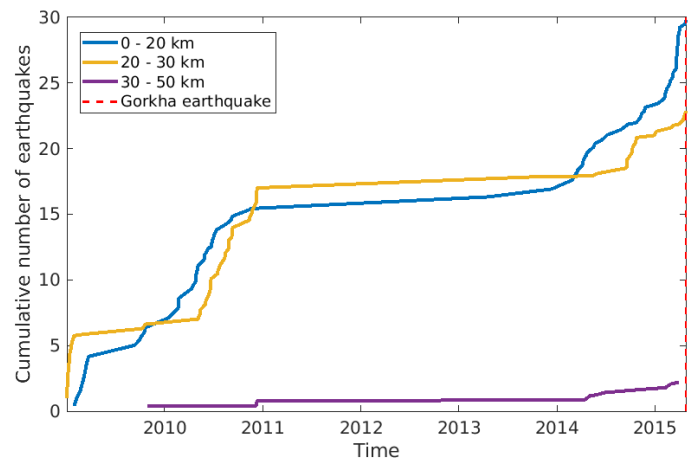


**Figure 6** Cumulative number of the background earthquakes according to their distance to Gorkha epicenter. The increase of seismic activity one month before the mainshock at distances between 0 and 20km is clearly seen in the background seismicity.

after a change point and it is based on a null hypothesis of stationarity (equality of observed rates before and after the change point). We apply it by taking a change point on a ten days moving window.

The change can be considered as significant if  $|Z| > 2$  (Marsan and Wyss, 2011).  $Z$  is greater than 2 for the entire catalogue and for the 0-20 km declustered catalogue, except at the end of the period where we see a drop off due to the lack of data (Supplementary Figure S13). This shows that, according to this statistic, the acceleration is significant, even after declustering.

In order to discriminate clusters as swarms or Mainshock-Aftershock (MS-AS) sequences, we compute the skewness of seismic moment release in each cluster (Roland and McGuire, 2009; Chen and Shearer, 2011; Zhang and Shearer, 2016; Passarelli et al., 2018) and the kurtosis (Mesimeri et al., 2019). The relationship between the skewness and the kurtosis leads to a parabola where MS-AS and swarms are clearly distinguished (Supplementary Figure S14). The results show that all our clusters (orange stars) can be characterized as swarms rather than Mainshock-Aftershock sequences.

## 6 Discussion

Although they can only be defined after the mainshock has occurred, seismic foreshocks are the most relevant observations for understanding the preparation of large earthquakes. We find 25 swarms of earthquakes that occurred before the Gorkha earthquake and that highlight the perimeter of its western coseismic slip area, where the rupture initiated. Several clusters have very-short durations and the longest and most important one in number of events occurs only one month before the Gorkha earthquake. This is the first time that a local, pre-seismic phase is evidenced in a context of collision such as the Himalayas.

Depending on the tectonic setting and structural complexity, three main conceptual models have been developed to explain the pre-seismic phase of large earthquakes: progressive localization of the seismicity, cascade-up, and pre-slip (Bouchon et al., 2011; Gombert, 2018; Ellsworth and Bulut, 2018; Kato and Ben-Zion, 2020; Ben-Zion and Zaliapin, 2020; Martínez-Garzón and Poli, 2024, and references therein).

Interestingly, for many large earthquakes that are preceded by a pre-seismic phase, the strain release is progressive, stepwise (Kato et al., 2012; Kato and Nakagawa, 2014; Socquet et al., 2017; Ruiz et al., 2014; Nishikawa and Ide, 2018). This is also noteworthy in this study, where we detect several seismic swarms that can be sudden and last only a few hours (Fig 2 bottom). Fluids may be a good candidate for triggering such events (Lengliné et al., 2017).

There are multiple indications of fluid presence in the area along the Main Himalayan Thrust (MHT): (a) a seismic low velocity zone (LVZ) coincides with the decollement on that particular section (Duputel et al., 2016), (b) this LVZ is interpreted as a shear zone possibly injected with fluids coming from metamorphic dehydration reactions of sediments thrust over by the hot Himalayan

hangingwall, (c) analysis of fluid inclusions from quartz exudates taken within the MCT shear zone, which is a former MHT, demonstrate that both aqueous fluids - mainly brines-, and  $CO_2$ -bearing inclusions, originating from metamorphic and meteoric origins, were introduced from mid-crustal to shallower levels (Boullier et al., 1991), (d) the downdip end of the segment of MHT considered corresponds with the position of a low-resistivity anomaly (Lemonnier et al., 1999), possibly attributed to the presence of saline fluids within fractured rocks.

This body of evidence suggests that aqueous fluids - or supercritical  $CO_2$  - are present at midcrustal depths in the vicinity of the decollement, with the potential to migrate within the fractured rocks of the shear zone as well as along subsidiary faults in its immediate hangingwall (Laporte et al., 2021). These fluid migrations could be related to hydrofracturation mechanisms and/or decrease of the friction on the basal decollement, possibly associated to transient decoupling.

The repeating earthquakes, associated to earthquake templates that happened at mid-crustal depths, occurred necessarily at close distances from the Main Himalayan Thrust, the flat-ramp-flat thrust system which partially ruptured during the mainshock (Fig. 7a-b). In this part of the Himalayas, the geometry of these structures at depth have been inferred from surface exposure of the rocks, (Ghoshal et al., 2023; Adhikari et al., 2022) and balanced cross section hypothesis. The position of the upper decollement of the thrust system is associated to the low velocity zone (LVZ) imaged by receiver function analysis (Nábělek et al., 2009; Duputel et al., 2016). Such a LVZ has been observed in other parts of the Himalayas, such as in the western Nepal with receiver functions (Subedi et al., 2018).

A first plausible scenario involves a transient slow slip seen in the declustered seismicity and with repeating earthquakes on the upper decollement, followed by its partial rupture, from the downdip end of the upper decollement, at the upper edge of the ramp (Fig. 7a-b). The average position of the ramp, at geological timescales, is suspected to develop beneath the front of the high Himalayas. This is consistent with the thermokinematic evolution recorded by the low temperature thermochronometers (e.g., Ghoshal et al., 2023). However, the present day position of the peak of uplift measured by InSAR and the peak of incision estimated along the rivers since the beginning of the Holocene suggest that the midcrustal ramp recently migrated southward (Grandin et al., 2012, see Fig. 7c). An alternative to the first scenario could therefore involve the rupture of this active midcrustal ramp, after a focused repetitive seismic activity at the updip end of the ramp, eventually associated with a slow slip event at the edge of the ramp. A third scenario involves seismicity in the midcrustal lesser Himalaya duplex. This scenario may involve a focused precursory seismic activity associated with an eventual slow slip at the updip edge of the active ramp, followed by the rupture of the passive roof thrust of the lesser Himalayan duplex (Fig. 7c). The alternative models illustrated in Fig. 7 are difficult to differentiate with the sole seismicity available due to the

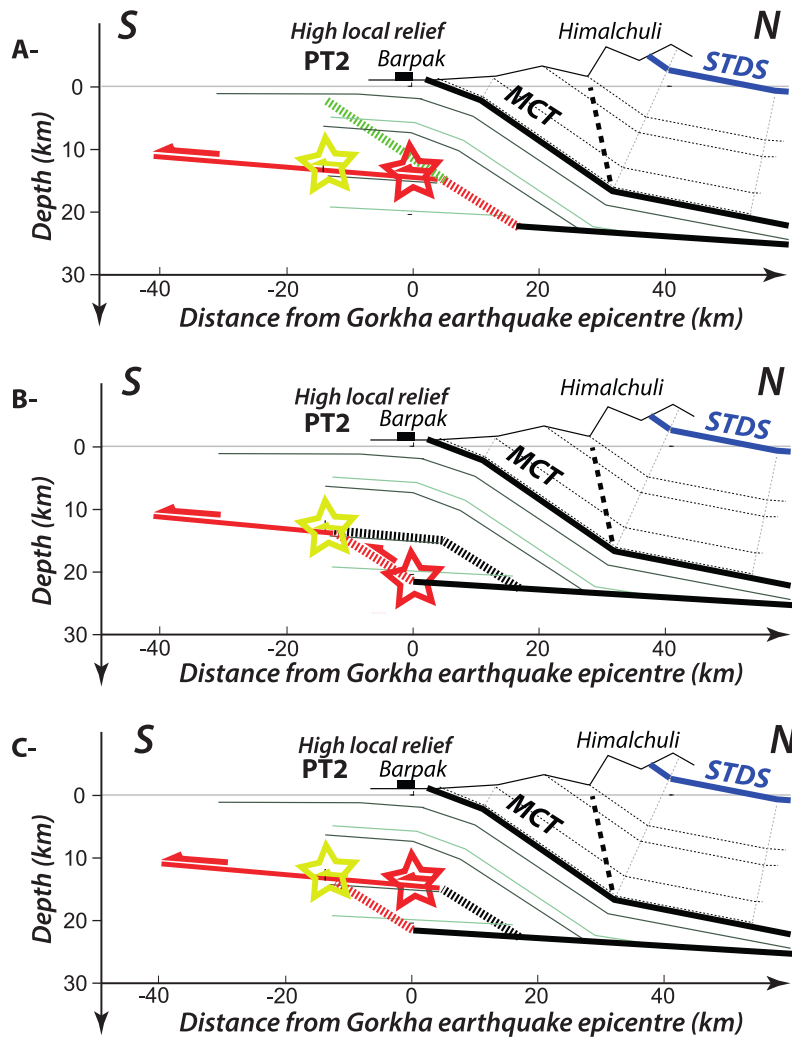


**Figure 7** Schematic representation of possible hypotheses regarding the location of the onset of the Gorkha earthquake rupture (red star) and the main cluster prior to the earthquake (yellow star). A- B and C respectively illustrate a scenario involving the rupture of the upper flat (A) of the Main Himalayan Thrust system (MHT), of the upper flat and a mid-crustal ramp (B), and of the passive roof thrust of the MHT (C). The red circles correspond to the location of the earthquakes which were selected as templates. Note that the hypocentral locations of these small earthquakes in the area are associated with very large uncertainties and need to be taken with care: the seismic stations that participate to their location are present to the south of the seismic swarm, leaving large primary azimuthal gaps. The geological structures are constrained by field observations (derived from structural measures of the bedding and schistosity), modified from [Adhikari et al. \(2022\)](#). MCT, STDS and PT2 respectively stand for Main Central Thrust, Southern Tibetan detachment system, and Physiographic transition 2.

large uncertainties associated with the earthquake locations.

## 7 Conclusion

The application of template matching techniques to the waveforms of the GKN station, the closest station to the epicenter of the Gorkha earthquake, confirms a previous observation ([Huang et al., 2017](#)) of an acceleration of the seismicity rate preceding the earthquake. In addition, we show that this acceleration is concentrated within 20 km from the mainshock.

Several seismic swarms occurred during the analysed period. Some of them have very short-term duration. The most important cluster is detected by two very close by and highly similar templates between the 20 March

and 27 March 2015, with 38 repeating earthquakes. This period is followed by the occurrence of at least one foreshock that happened 28s before the mainshock. This seismicity increase is seen in the declustered part of the catalogue meaning that it is sensitive to a local change of tectonic loading, most probably due to a transient slow slip event that is consistent with the occurrence of possible repeating micro-earthquakes happening at the north western edge of the rupture zone. There was a small earthquake that occurred a few seconds before the mainshock and it was finally followed by the rupture of the mainshock. With an estimation of 20 km for the radius of the foreshock area, the Gorkha earthquake ( $M_o = 7.7 \times 10^{20}$  N m, [Grandin et al., 2015](#)), would be consistent with the relationship proposed by [Martínez-Garzón and Poli \(2024\)](#) relating the size of the area ac-

tivated in a pre-seismic phase and the mainshock seismic moment. Our results show that the Gorkha earthquake belongs to the list of large earthquakes with a pre-seismic phase detected a posteriori using data mining techniques.

## Acknowledgements

We acknowledge the cooperation of the Department of Mines and Geology (DMG) - Nepal and CEA/DASE France in the maintenance of the seismological stations used in this study. We are grateful to the team of analysts at NEMRC/DMG, and to Section Chief Bharat Koirala, for their involvement in the processing of the seismicity catalogue. This study was initiated during Lok Bijaya Adhikari's doctoral thesis on the aftershocks of the Gorkha earthquake. **Funding:** BG postdoctoral fellowship was supported by the LRC Yves Rocard (Laboratoire de Recherche Conventionné CEA-ENS- CNRS).

## Data availability

Obspy's documentation is found at [docs.obspy.org](https://docs.obspy.org). The code repository, issue tracker, and general development can be found on [github.com/obspy/obspy](https://github.com/obspy/obspy) (Beyreuther et al., 2010). The catalogue presented in this article can be found in this repository : [github.com/gardonib/TM\\_NEPAL](https://github.com/gardonib/TM_NEPAL). Waveforms from the KKN broadband station are open access, made available in real time by the DMG/DASE collaboration on the IRIS/PASSCAL website under NK.KKN. Waveforms from the GKN station, property of the Department of Mines and Geology, Nepal, are available upon requests. This institute has a policy of making data available on the basis of 'specific requests' excluding the distribution to 'third parties' ([www.seismonepal.gov.np/](http://www.seismonepal.gov.np/)). DMG requires the completion of a request form at [seismonepal.gov.np](http://seismonepal.gov.np).

## Competing interests

The authors declare no competing interests.

## References

- Adhikari, L., Gautam, U., Koirala, B., Bhattarai, M., Kandel, T., Gupta, R., Timsina, C., Maharjan, N., Maharjan, K., Dahal, T., Hoste-Colomer, R., Cano, Y., Dandine, M., Guilhem, A., Merrer, S., Roudil, P., and Bollinger, L. The aftershock sequence of the 2015 April 25 Gorkha–Nepal earthquake. *Geophysical Journal International*, 203(3):2119–2124, Dec. 2015. doi: 10.1093/gji/ggv412.
- Adhikari, L. B., Laporte, M., Bollinger, L., Vergne, J., Lambotte, S., Koirala, B. P., Bhattarai, M., Timsina, C., Gupta, R. M., Wendling-Vazquez, N., Batteux, D., Lyon-Caen, H., Gaudemer, Y., Bernard, P., and Perrier, F. Seismically active structures of the Main Himalayan Thrust revealed before, during and after the 2015 *M* 7.9 Gorkha earthquake in Nepal. *Geophysical Journal International*, 232(1):451–471, Oct. 2022. doi: 10.1093/gji/ggac281.
- Avouac, J.-P. Mountain building, erosion, and the seismic cycle in the Nepal Himalaya. *Advances in geophysics*, 46:1–80, 2003.
- Avouac, J.-P., Meng, L., Wei, S., Wang, T., and Ampuero, J.-P. Lower edge of locked Main Himalayan Thrust unzipped by the 2015 Gorkha earthquake. *Nature Geoscience*, 8(9):708–711, Sept. 2015. doi: 10.1038/ngeo2518.
- Bai, L., Klemperer, S. L., Mori, J., Karplus, M. S., Ding, L., Liu, H., Li, G., Song, B., and Dhakal, S. Lateral variation of the Main Himalayan Thrust controls the rupture length of the 2015 Gorkha earthquake in Nepal. *Science Advances*, 5(6):eaav0723, June 2019. doi: 10.1126/sciadv.aav0723.
- Baillard, C., Lyon-Caen, H., Bollinger, L., Rietbrock, A., Letort, J., and Adhikari, L. B. Automatic analysis of the Gorkha earthquake aftershock sequence: evidences of structurally segmented seismicity. *Geophysical Journal International*, 209(2):1111–1125, May 2017. doi: 10.1093/gji/ggx081.
- Ben-Zion, Y. and Zaliapin, I. Localization and coalescence of seismicity before large earthquakes. *Geophysical Journal International*, 223(1):561–583, Oct. 2020. doi: 10.1093/gji/ggaa315.
- Beyreuther, M., Barsch, R., Krischer, L., Megies, T., Behr, Y., and Wassermann, J. ObsPy: A Python toolbox for seismology. *Seismological Research Letters*, 81(3):530–533, 2010.
- Bilham, R. Location and magnitude of the 1833 Nepal earthquake and its relation to the rupture zones of contiguous great Himalayan earthquakes. *Current Science*, 69(2):101–128, 1995. <https://www.jstor.org/stable/24097233>.
- Bilham, R. Himalayan earthquakes: a review of historical seismicity and early 21st century slip potential. *Geological Society, London, Special Publications*, 483(1):423–482, Jan. 2019. doi: 10.1144/SP483.16.
- Bouchon, M., Karabulut, H., Aktar, M., Özalaybey, S., Schmittbuhl, J., and Bouin, M.-P. Extended Nucleation of the 1999 Mw 7.6 Izmit Earthquake. *Science*, 331(6019):877–880, Feb. 2011. doi: 10.1126/science.1197341.
- Bouchon, M., Durand, V., Marsan, D., Karabulut, H., and Schmittbuhl, J. The long precursory phase of most large interplate earthquakes. *Nature Geoscience*, 6(4):299–302, Apr. 2013. doi: 10.1038/ngeo1770.
- Bouchon, M., Marsan, D., Durand, V., Campillo, M., Perfettini, H., Madariaga, R., and Gardonio, B. Potential slab deformation and plunge prior to the Tohoku, Iquique and Maule earthquakes. *Nature Geoscience*, 9(5):380–383, May 2016. doi: 10.1038/ngeo2701.
- Bouchon, M., Socquet, A., Marsan, D., Guillot, S., Durand, V., Gardonio, B., Campillo, M., Perfettini, H., Schmittbuhl, J., Renard, F., and Boullier, A.-M. Observation of rapid long-range seismic bursts in the Japan Trench subduction leading to the nucleation of the Tohoku earthquake. *Earth and Planetary Science Letters*, 594:117696, Sept. 2022. doi: 10.1016/j.epsl.2022.117696.
- Boullier, A.-M., France-Lanord, C., Dubessy, J., Adamy, J., and Champenois, M. Linked fluid and tectonic evolution in the High Himalaya mountains (Nepal). *Contributions to Mineralogy and Petrology*, 107(3):358–372, May 1991. doi: 10.1007/BF00325104.
- Chen, X. and Shearer, P. Comprehensive analysis of earthquake source spectra and swarms in the Salton Trough, California. *Journal of Geophysical Research: Solid Earth*, 116(B9), 2011.
- Duputel, Z., Vergne, J., Rivera, L., Wittlinger, G., Farra, V., and Hétényi, G. The 2015 Gorkha earthquake: A large event illuminating the Main Himalayan Thrust fault. *Geophysical Research Letters*, 43(6):2517–2525, Mar. 2016. doi: 10.1002/2016GL068083.
- Ellsworth, W. L. and Bulut, F. Nucleation of the 1999 Izmit earthquake by a triggered cascade of foreshocks. *Nature Geoscience*, 11(7):531–535, July 2018. doi: 10.1038/s41561-018-0145-1.
- Galetzka, J., Melgar, D., Genrich, J. F., Geng, J., Owen, S., Lindsey, E. O., Xu, X., Bock, Y., Avouac, J.-P., Adhikari, L. B., Upreti, B. N., Pratt-Sitaula, B., Bhattarai, T. N., Sitaula, B. P., Moore, A., Hudnut, K. W., Szeliga, W., Normandeau, J., Fend, M., Flouzat, M.,

- Bollinger, L., Shrestha, P., Koirala, B., Gautam, U., Bhattarai, M., Gupta, R., Kandel, T., Timsina, C., Sapkota, S. N., Rajaura, S., and Maharjan, N. Slip pulse and resonance of the Kathmandu basin during the 2015 Gorkha earthquake, Nepal. *Science*, 349(6252): 1091–1095, Sept. 2015. doi: 10.1126/science.aac6383.
- Gardner, J. and Knopoff, L. Is the sequence of earthquakes in Southern California, with aftershocks removed, Poissonian? *Bulletin of the seismological society of America*, 64(5):1363–1367, 1974.
- Gardonio, B., Jolivet, R., Calais, E., and Leclère, H. The April 2017 Mw6.5 Botswana Earthquake: An Intraplate Event Triggered by Deep Fluids. *Geophysical Research Letters*, 45(17):8886–8896, 2018. doi: 10.1029/2018GL078297.
- Gardonio, B., Campillo, M., Marsan, D., Lecointre, A., Bouchon, M., and Letort, J. Seismic Activity Preceding the 2011 Mw9.0 Tohoku Earthquake, Japan, Analyzed With Multidimensional Template Matching. *Journal of Geophysical Research: Solid Earth*, 124(7): 6815–6831, 2019. doi: 10.1029/2018JB016751.
- Ghoshal, S., McQuarrie, N., Huntington, K. W., Robinson, D. M., and Ehlers, T. A. Testing erosional and kinematic drivers of exhumation in the central Himalaya. *Earth and Planetary Science Letters*, 609:118087, May 2023. doi: 10.1016/j.epsl.2023.118087.
- Gomberg, J. Unsettled earthquake nucleation. *Nature Geoscience*, 11(7):463–464, July 2018. doi: 10.1038/s41561-018-0149-x.
- Grandin, R., Doin, M.-P., Bollinger, L., Pinel-Puysségur, B., Ducret, G., Jolivet, R., and Sapkota, S. N. Long-term growth of the Himalaya inferred from interseismic InSAR measurement. *Geology*, 40(12):1059–1062, Dec. 2012. doi: 10.1130/G33154.1.
- Grandin, R., Vallée, M., Satriano, C., Lacassin, R., Klinger, Y., Simoes, M., and Bollinger, L. Rupture process of the  $M_w = 7.9$  2015 Gorkha earthquake (Nepal): Insights into Himalayan megathrust segmentation: RUPTURE PROCESS OF THE GORKHA EARTHQUAKE. *Geophysical Research Letters*, 42(20):8373–8382, Oct. 2015. doi: 10.1002/2015GL066044.
- Gualandi, A., Avouac, J.-P., Galetzka, J., Genrich, J. F., Blewitt, G., Adhikari, L. B., Koirala, B. P., Gupta, R., Upreti, B. N., Pratt-Sitaula, B., and Liu-Zeng, J. Pre- and post-seismic deformation related to the 2015,  $M_w 7.8$  Gorkha earthquake, Nepal. *Tectonophysics*, 714-715:90–106, Sept. 2017. doi: 10.1016/j.tecto.2016.06.014.
- Habermann, R. Precursory seismicity patterns: Stalking the mature seismic gap. *Earthquake prediction: An international review*, 4:29–42, 1981.
- Hainzl, S. and Marsan, D. Dependence of the Omori-Utsu law parameters on main shock magnitude: Observations and modeling. *Journal of Geophysical Research: Solid Earth*, 113(B10), 2008.
- Hainzl, S., Zakharova, O., and Marsan, D. Impact of aseismic transients on the estimation of aftershock productivity parameters. *Bulletin of the Seismological Society of America*, 103(3): 1723–1732, 2013.
- Hoste-Colomer, R., Bollinger, L., Lyon-Caen, H., Burtin, A., and Adhikari, L. Lateral structure variations and transient swarm revealed by seismicity along the Main Himalayan Thrust north of Kathmandu. *Tectonophysics*, 714-715:107–116, Sept. 2017. doi: 10.1016/j.tecto.2016.10.004.
- Huang, H., Meng, L., Plasencia, M., Wang, Y., Wang, L., and Xu, M. Matched-filter detection of the missing pre-mainshock events and aftershocks in the 2015 Gorkha, Nepal earthquake sequence. *Tectonophysics*, 714:71–81, 2017.
- Kato, A. and Ben-Zion, Y. The generation of large earthquakes. *Nature Reviews Earth & Environment*, 2(1):26–39, Nov. 2020. doi: 10.1038/s43017-020-00108-w.
- Kato, A. and Nakagawa, S. Multiple slow-slip events during a foreshock sequence of the 2014 Iquique, Chile Mw 8.1 earthquake. *Geophysical Research Letters*, 41(15):5420–5427, 2014. doi: 10.1002/2014GL061138.
- Kato, A., Obara, K., Igarashi, T., Tsuruoka, H., Nakagawa, S., and Hirata, N. Propagation of Slow Slip Leading Up to the 2011 Mw 9.0 Tohoku-Oki Earthquake. *Science*, 335(6069):705–708, Feb. 2012. doi: 10.1126/science.1215141.
- Kobayashi, T., Morishita, Y., and Yurai, H. Detailed crustal deformation and fault rupture of the 2015 Gorkha earthquake, Nepal, revealed from ScanSAR-based interferograms of ALOS-2. *Earth, Planets and Space*, 67(1):201, Dec. 2015. doi: 10.1186/s40623-015-0359-z.
- Koirala, B. P., Laporte, M., Bollinger, L., Batteux, D., Letort, J., Guilhem Trilla, A., Wendling-Vazquez, N., Bhattarai, M., Subedi, S., and Adhikari, L. B. Tectonic significance of the 2021 Lamjung, Nepal, mid-crustal seismic cluster. *Earth, Planets and Space*, 75(1):165, Oct. 2023. doi: 10.1186/s40623-023-01888-3.
- Laporte, M. Contribution à l'amélioration de l'estimation de la profondeur hypocentrale à partir de réseaux régionaux ou globaux, 2022.
- Laporte, M., Bollinger, L., Lyon-Caen, H., Hoste-Colomer, R., Duverger, C., Letort, J., Riesner, M., Koirala, B. P., Bhattarai, M., Kandel, T., Timsina, C., and Adhikari, L. B. Seismicity in far western Nepal reveals flats and ramps along the Main Himalayan Thrust. *Geophysical Journal International*, 226(3):1747–1763, Sept. 2021. doi: 10.1093/gji/ggab159.
- Larsonnier, F., Rouillé, G., Bartoli, C., Klaus, L., and Begoff, P. Comparison on seismometer sensitivity following ISO 16063-11 standard, 2019.
- Lemonnier, C., Marquis, G., Perrier, F., Avouac, J.-P., Chitrakar, G., Kafle, B., Sapkota, S., Gautam, U., Tiwari, D., and Bano, M. Electrical structure of the Himalaya of central Nepal: High conductivity around the mid-crustal ramp along the MHT. *Geophysical Research Letters*, 26(21):3261–3264, 1999. doi: 10.1029/1999GL008363.
- Lengliné, O., Boubacar, M., and Schmittbuhl, J. Seismicity related to the hydraulic stimulation of GRT1, Rittershoffen, France. *Geophysical Journal International*, 208(3):1704–1715, Mar. 2017. doi: 10.1093/gji/ggw490.
- Letort, J., Bollinger, L., Lyon-Caen, H., Guilhem, A., Cano, Y., Bailard, C., and Adhikari, L. B. Teleseismic depth estimation of the 2015 Gorkha Nepal aftershocks. *Geophysical Journal International*, 207(3):1584–1595, Dec. 2016. doi: 10.1093/gji/ggw364.
- Lindsey, E. O., Natsuaki, R., Xu, X., Shimada, M., Hashimoto, M., Melgar, D., and Sandwell, D. T. Line-of-sight displacement from ALOS-2 interferometry: Mw 7.8 Gorkha Earthquake and Mw 7.3 aftershock. *Geophysical Research Letters*, 42(16):6655–6661, 2015. doi: 10.1002/2015GL065385.
- Lindsey, E. O., Almeida, R., Mallick, R., Hubbard, J., Bradley, K., Tsang, L. L., Liu, Y., Burgmann, R., and Hill, E. M. Structural control on downdip locking extent of the Himalayan megathrust. *Journal of Geophysical Research: Solid Earth*, 123(6):5265–5278, 2018.
- Marsan, D. and Lengline, O. Extending earthquakes' reach through cascading. *Science*, 319(5866):1076–1079, 2008.
- Marsan, D. and Wyss, M. Seismicity rate changes. *Community Online Resource for Statistical Seismicity Analysis*, 2011.
- Martin, S. S., Hough, S. E., and Hung, C. Ground Motions from the 2015 Mw 7.8 Gorkha, Nepal, Earthquake Constrained by a Detailed Assessment of Macroseismic Data. *Seismological Research Letters*, 86(6):1524–1532, Nov. 2015. doi: 10.1785/0220150138.

- Martínez-Garzón, P. and Poli, P. Cascade and pre-slip models oversimplify the complexity of earthquake preparation in nature. *Communications Earth & Environment*, 5(1):120, 2024.
- Mendoza, M. M., Ghosh, A., Karplus, M. S., Klemperer, S. L., Sapkota, S. N., Adhikari, L. B., and Velasco, A. Duplex in the Main Himalayan Thrust illuminated by aftershocks of the 2015 Mw 7.8 Gorkha earthquake. *Nature Geoscience*, 12(12):1018–1022, Dec. 2019. doi: 10.1038/s41561-019-0474-8.
- Mesimeri, M., Karakostas, V., Papadimitriou, E., and Tsaklidis, G. Characteristics of earthquake clusters: Application to western Corinth Gulf (Greece). *Tectonophysics*, 767:228160, 2019.
- Mignan, A. The debate on the prognostic value of earthquake foreshocks: A meta-analysis. *Scientific reports*, 4(1):4099, 2014.
- Nandan, S., Ouillon, G., Wiemer, S., and Sornette, D. Objective estimation of spatially variable parameters of epidemic type aftershock sequence model: Application to California. *Journal of Geophysical Research: Solid Earth*, 122(7):5118–5143, 2017.
- Nishikawa, T. and Ide, S. Recurring Slow Slip Events and Earthquake Nucleation in the Source Region of the M 7 Ibaraki-Oki Earthquakes Revealed by Earthquake Swarm and Foreshock Activity. *Journal of Geophysical Research: Solid Earth*, 123(9):7950–7968, 2018. doi: 10.1029/2018JB015642.
- Nábělek, J., Hetényi, G., Vergne, J., Sapkota, S., Kafle, B., Jiang, M., Su, H., Chen, J., Huang, B.-S., and Team, t. H.-C. Underplating in the Himalaya-Tibet Collision Zone Revealed by the Hi-CLIMB Experiment. *Science*, 325(5946):1371–1374, Sept. 2009. doi: 10.1126/science.1167719.
- Ogata, Y. Statistical models for earthquake occurrences and residual analysis for point processes. *Journal of the American Statistical Association*, 83(401):9–27, 1988.
- Pandey, M. R. Seismic model of central and eastern Lesser Himalaya of Nepal. *Journal of Nepal Geological Society*, 3:1–11, Dec. 1985. doi: 10.3126/jngs.v3i0.32655.
- Passarelli, L., Rivalta, E., Jónsson, S., Hensch, M., Metzger, S., Jakobsdóttir, S. S., Maccaferri, F., Corbi, F., and Dahm, T. Scaling and spatial complementarity of tectonic earthquake swarms. *Earth and Planetary Science Letters*, 482:62–70, 2018.
- Riesner, M., Bollinger, L., Rizza, M., Klinger, Y., Karakaş, c., Sapkota, S. N., Shah, C., Guérin, C., and Tapponnier, P. Surface rupture and landscape response in the middle of the great Mw 8.3 1934 earthquake mesoseismal area: Khutti Khola site. *Scientific Reports*, 13(1):4566, Mar. 2023. doi: 10.1038/s41598-023-30697-7.
- Roland, E. and McGuire, J. J. Earthquake swarms on transform faults. *Geophysical Journal International*, 178(3):1677–1690, 2009.
- Ruiz, S., Metois, M., Fuenzalida, A., Ruiz, J., Leyton, F., Grandin, R., Vigny, C., Madariaga, R., and Campos, J. Intense foreshocks and a slow slip event preceded the 2014 Iquique Mw 8.1 earthquake. *Science*, 345(6201):1165–1169, Sept. 2014. doi: 10.1126/science.1256074.
- Socquet, A., Valdes, J. P., Jara, J., Cotton, F., Walpersdorf, A., Cotte, N., Specht, S., Ortega-Culaciati, F., Carrizo, D., and Norabuena, E. An 8 month slow slip event triggers progressive nucleation of the 2014 Chile megathrust. *Geophysical Research Letters*, 44(9):4046–4053, 2017. doi: 10.1002/2017GL073023.
- Subedi, S., Hetényi, G., Vergne, J., Bollinger, L., Lyon-Caen, H., Farra, V., Adhikari, L. B., and Gupta, R. M. Imaging the Moho and the Main Himalayan Thrust in Western Nepal with receiver functions. *Geophysical Research Letters*, 45(24):13–222, 2018.
- Utsu, T., Ogata, Y., et al. The centenary of the Omori formula for a decay law of aftershock activity. *Journal of Physics of the Earth*, 43(1):1–33, 1995.
- Wang, X., Wei, S., and Wu, W. Double-ramp on the Main Himalayan Thrust revealed by broadband waveform modeling of the 2015 Gorkha earthquake sequence. *Earth and Planetary Science Letters*, 473:83–93, Sept. 2017. doi: 10.1016/j.epsl.2017.05.032.
- Wesnousky, S. G., Kumahara, Y., Chamlagain, D., Pierce, I. K., Karki, A., and Gautam, D. Geological observations on large earthquakes along the Himalayan frontal fault near Kathmandu, Nepal. *Earth and Planetary Science Letters*, 457:366–375, Jan. 2017. doi: 10.1016/j.epsl.2016.10.006.
- Yamada, M., Kandel, T., Tamaribuchi, K., and Ghosh, A. 3D Fault Structure Inferred from a Refined Aftershock Catalog for the 2015 Gorkha Earthquake in Nepal. *Bulletin of the Seismological Society of America*, 110(1):26–37, Nov. 2019. doi: 10.1785/0120190075.
- Zaliapin, I. and Ben-Zion, Y. Perspectives on clustering and declustering of earthquakes. *Seismological Research Letters*, 93(1):386–401, 2022.
- Zhang, Q. and Shearer, P. M. A new method to identify earthquake swarms applied to seismicity near the San Jacinto Fault, California. *Geophysical Journal International*, 205(2):995–1005, 2016.
- Zhao, B., Bürgmann, R., Wang, D., Tan, K., Du, R., and Zhang, R. Dominant Controls of Downdip Afterslip and Viscous Relaxation on the Postseismic Displacements Following the Mw7.9 Gorkha, Nepal, Earthquake. *Journal of Geophysical Research: Solid Earth*, 122(10):8376–8401, 2017. doi: 10.1002/2017JB014366.

The article *Seismicity acceleration and clustering before the 2015  $M_w$  7.9 Gorkha earthquake, Nepal* © 2025 by B. Gardonio is licensed under CC BY 4.0.